Scientific Reports

https://doi.org/10.1038/s41598-026-54063-5

Article in Press

Longitudinal tracking of dyadic body temperature synchrony in social pairs across species

Received: 20 June 2025

Accepted: 16 May 2026

Published online: 27 May 2026

Cite this article as: Yazaki-Sugiyama Y., Makino Y., Isogai R. *et al.* Longitudinal tracking of dyadic body temperature synchrony in social pairs across species. *Sci Rep* (2026). https://doi.org/10.1038/s41598-026-54063-5

Yoko Yazaki-Sugiyama, Yuichi Makino, Ryosuke Isogai, Yudai Imano, Minghao Nie, Masafumi Kuroda, Kotaro Maki, Shoji Takeuchi, Yoshifumi Yoshida & Takao K. Hensch

Title: Longitudinal tracking of dyadic body temperature synchrony in social pairs across species

Authors: Yoko Yazaki-Sugiyama[1,2]*, Yuichi Makino[2], Ryosuke Isogai[3], Yudai Imano[3], Minghao Nie[4], Masafumi Kuroda[2], Kotaro Maki[5], Shoji Takeuchi[2,4], Yoshifumi Yoshida[3], Takao K. Hensch[2,6]

[1]Neuronal Mechanism for Critical Period Unit, OIST Graduate University, Okinawa,

904-0495, Japan

[2]International Research Center for Neurointelligence, The University of Tokyo, 103-0033, Tokyo,

[3]Seiko Future Creation Inc., Chiba, 279-2222, Japan,

[4]Graduate School of Information Science and Technology, The University of Tokyo, Tokyo, 103-0033, Japan

[5]School of Dentistry, Showa University Tokyo, 142-8555 Japan,

[6]Molecular Cellular Biology, Harvard University, Cambridge, MA 02138, USA

***Corresponding author:** yazaki-sugiyama@oist.jp

Abstract (200 words)

Social behavior shapes efficient vocal communication and broadly impacts our mental health. While social interactions have been suggested to

synchronize daily rhythmicity or even brain activity, examining biophysical signals across naturally behaving individuals in a non-intrusive manner remains challenging. Here, we developed a lightweight, miniature wireless thermo-sensor device and implanted it subcutaneously in pairs of mice or zebra finches to track body temperature fluctuations continuously in their home cages. In both species, longitudinal monitoring revealed increased body temperature synchrony between co-housed pairs despite differing social contexts. Notably, Spearman correlation coefficients differed most during huddled sleep phases, being higher in nocturnal mice and lower in diurnal zebra finches when compared to their active social interactions during waking. Our innovative wearable thermo-sensors provide a powerful new tool for further investigating underlying brain mechanisms when combined with simultaneous monitoring of neuronal activity to inspire translatable biomarkers for clinical targets and improved methods for efficient social learning. (153 words)

Keywords

Social synchrony; Social interaction; miniature biosensor device;

Introduction

Interactions with conspecific individuals have substantial impacts on physical and mental well-being. Especially in early life, humans and animals acquire new skills, like vocal communication, by socially engaging with adult tutors (1-3). In turn, early life stress, such as parental neglect, can disrupt functional brain development leading to psychiatric illness (4-6). Both chronic stress in

rodents and enduring depression in humans further dysregulate body temperature (7, 8).

Social synchrony in circadian or menstrual rhythmicity has been reported in humans, animals, and insects (9-13). While the involvement of sensory (olfactory) cues has been suggested (9, 14), underlying mechanisms of social synchrony are still largely unknown. Recent studies using wireless devices further revealed that synchronized brain activity emerges within social dyads under semi-natural conditions (3, 15-17). Together, these findings suggest that the impact of social life can be tracked by the longitudinal measurement of biophysical signals, such as body temperature. However, it has been challenging to pursue in a non-intrusive manner that does not disrupt group dynamics.

Here, we developed a small, wireless, subcutaneously implantable thermo-sensor device and measured body temperature of mouse male and zebra finch mating pairs socially interacting in their home cages (Fig. 1). Our longitudinal monitoring of body temperature revealed synchronous fluctuation among social pairs in different contexts and species. We further found dramatic differences in sleep synchrony between mammalian and avian species.

Results

To demonstrate the value of simultaneous dyadic physiological tracking, we longitudinally examined three distinct contexts in two small animal models: 1) same-sex peer pairs of adult male mice; 2) male-female courtship pairs of

zebra finches; and 3) active sleep bouts between awake periods. High-resolution continuous body temperature measurements were obtained during naturalistic interactions over several days at various stages of co-housing using a novel wireless implantable device (Fig 1A). This sensor features miniaturized components, onboard memory storage, optically-triggered Bluetooth connection and ultra-low power consumption technology (Fig. 1 B & C) enabling recording from multiple freely behaving individuals in their home cages.

Social synchrony of body temperature in male mouse pairs

With the device implanted subcutaneously and left uninterrupted (data stored to device), male mouse pairs behaved naturally without noticeable aggression over the entire recording period (for 3-8 days after co-housing; Fig. 2A). Daily rhythms of body temperature were observed, consistent with the nocturnal activity profile of rodents, but unconfirmed as circadian rhythmicity by further recording under constant dark conditions (Fig. 2B). To initially avoid this intrinsic timer, we examined correlations of body temperature over a full 24-hour period excluding the one hour before and after lights switched on/off, then subtracted the average for each individual across days (delta body temperature).

Notably, we found that body temperature fluctuations across the light/dark cycle were synchronized for animals co-housed in the same cage. Spearman correlation coefficients of delta body temperature were significantly higher after housing together than when apart in separate cages

(Fig. 2C; p = 0.0063, df = 14.98, t-value = 4.30, Linear mixed model fit by maximum likelihood. t-tests use Satterthwaite's method [lmerModLmerTest]). Correlation strength was high soon after (< 1 day) pairing together and did not change depending on the length of housing (p > 0.05, r^2 = 0.014) (Fig. 2D, Supplemental Fig. 1), revealing immediate social synchrony of body temperature between same-sex peers housed in the same cage.

Social synchrony of body temperature in zebra finch mating pairs

The same miniature wireless thermo-sensor device was also successfully implanted in zebra finches (Fig. 3A). Male and female courtship pairs behaved naturally, including flight, for up to several weeks (8–19 days, 5 pairs, Supplemental Table 1) with minimal interruption (data extracted every 4–10 days while the device remained subcutaneously secure). Again, daily rhythmicity in body temperature was observed but with opposite polarity from mice, as expected for diurnally active zebra finches (Fig. 3B).

We also found synchronous body temperature fluctuations over the light/dark cycle between zebra finch mating pairs within the same cage but not across those from different cages simultaneously in the same room (i.e. male-female pairs were shuffled across those recorded concurrently in different cages and chambers), as indicated by significantly higher Spearman correlation coefficient (Fig. 3C; p = 0.044, df = 10.96, t-value = 2.28, lmerModLmerTest). While strength of correlation could vary across pairs, the effect of variation between pairs was not significant (p = 0.11, df = 13.20, t-

value = 1.72, lmerModLmerTest), and similar in average magnitude to that of mice (Fig. 2C).

Notably unlike same-sex mouse peers, synchrony strength increased only gradually across days after zebra finch courtship pairing (Fig. 3D, Supplemental Fig. 2), correlating positively as a group (pooled data from all pairs, $p = 0.025$, $r^2 = 0.079$) and specifically for one pair recorded over co-housing for several weeks (Fig. 3D, green triangles; $p = 0.0049$, $r^2 = 0.38$). The emergence rate of body temperature synchrony may thus reflect specific social conditions, such as mating (birds) or peer interactions (mice).

Species-specific sleep synchrony

As social contexts differed between species, we further analyzed the intervening non-socially active sleep periods. Mouse pairs huddled together during sleep, fragmented by synchronous, short bouts of waking movements. This was captured by cycles of dramatic peaks in pixel value differences of sequential video frames from two pairs, coinciding with a concurrent rise in body temperature for both mice (Fig. 4A, left; Supplemental Fig. 3). Visual inspection confirmed the mouse pairs huddled together for most of the sleep periods (>30 min) as reflected in lower frame differences (non-movement) (14/16 and 13/16 sleep periods for each pair over 2 nights).

Strikingly, Spearman correlation coefficients of body temperature between mouse pairs in the same cage were significantly higher when they were asleep (light phase) than when they were socially active (dark phase) (Fig. 4B, left; $p = 0.015$, df = 19.10, t-value = 2.67, lmerModLmerTest).

Further, distributions of correlation coefficients measured specifically during sleep periods without movement (i.e., lowest frame differences) did not differ from that over all nights (light phase) ($p = 0.58$, K-S test) and was higher than that for the awake period ($p = 0.021$, K-S test) (Fig. 4C, left). Thus, stronger body temperature synchrony was observed between mouse pairs when asleep independent of awake social activity.

Zebra finch pairs were confirmed to co-habit the nest during most of their sleep period (dark phase), again by visual inspection of video recordings (20/22 nights, 2–8 nights/5 pairs). Occasional head and tail movements in the nest were not synchronized, as suggested by only small differences in sequential video frames which did not correlate with body temperature fluctuations (Fig. 4A, right; Supplemental Fig. 3). As opposed to the mice, Spearman correlation coefficients between paired birds were significantly lower when asleep (dark phase) than when awake (light phase) (Fig. 4B right; $p < 0.0001$, df = 82.10, t-value = 5.22, lmerModLmerTest). The pairing duration, which predicted the gradual emergence of social synchrony (Fig. 3D), did not affect the difference in synchrony strength between asleep and awake periods ($p = 0.12$, df = 6.08, t-value = 1.83). Lower synchrony while nesting together asleep (as confirmed by video inspection) did not differ from that of the full dark phase ($p = 0.98$, Kolmogorov–Smirnov [K-S] test), which

was again less than that of the entire wake period (p = 0.027, K-S test) (Fig. 4C, right).

Taken together, our data indicate that both mouse and bird pairs sleep together by huddling, while their body temperature synchrony response compared to awake periods was diametrically opposite: increased in sleeping mice but reduced in sleeping birds. We therefore revisited the regulation of body temperature around the time of light onset/offset. Whereas mouse dyads were closely coupled to the Zeitgeber at these transitions (Fig. 5A), birds individually anticipated the circadian switching by 10-15 min (Fig. 5B), consistent with a closer adherence to an internal clock.

Discussion

Here, we developed a lightweight, miniature wireless sensor for continuous tracking of body temperature and observed synchronous dyadic fluctuations across pairs of mice or zebra finches that were naturally interacting in their home cages. While the social context differed across species (mouse male peers; male-female bird courtship pairs), both groups showed similar correlation coefficients when shared interactions were possible rather than socially apart. Notably, non-socially active sleep phases differentiated the peak strength of dyadic synchrony across the two species — being higher in sleeping mice and lower for sleeping birds (Fig 5C).

One possibility is that social context in waking might directly influence “mindset” during subsequent sleep when active social behavior ceases. Motivation for prolonged physical contact and synchronized brain activity

during sleep (“somatolonging”) was recently suggested for mice (17). Instead, in birds sleep weakened the synchrony promoted by active social engagement in waking, suggesting a differential effect by species and/or behavioral context. Body temperature is bidirectionally altered under stressful conditions in both humans and animals (6,7). Olfactory cues have been suggested to regulate social synchrony in *Drosophila* circadian rhythmicity (14) and human menstrual cycles (9). However, olfactory involvement is unlikely in the body temperature synchrony here, which occurred on a much faster timescale. Moreover, LMMs analysis revealed that bird synchrony strength differed significantly across day and night, unaffected by how long the pairs were housed together. This would dissociate their sleep synchrony from the gradually increasing social synchrony in these mating pairs (Fig. 3D).

Perhaps a more likely explanation for divergent sleep synchrony across species can be found in the mechanisms of mammalian and avian thermoregulation. In rodents, NREM–REM cycling is strongly linked to predictable fluctuations in body temperature that are coordinated by the suprachiasmatic nucleus and hypothalamic thermoregulatory centers. Higher synchrony during sleep with huddling in mice can be naturally explained as it involves shared thermoregulation (Fig. 5A) (18). Zebra finches also show tight coupling between sleep and thermoregulatory behavior. Their body temperature started to increase anticipatory to diurnal light switching. But in birds, their feathers insulate body heat from the outside with layers of

air. The reliance on evaporative cooling and rapid body temperature modulation at high temperatures introduces additional, idiosyncratic fluctuations not strictly tied to the partner's sleep state, thereby decorrelating pairwise body temperature signals (Fig. 5B).

Synchronous brain activity in socially interacting animal groups (10, 11, 17) and the cues used for synchronized circadian rhythms seem to vary between animal species (reviewed in 19). Circadian fluctuations of brain temperature in humans have also been reported (20) and are elevated in clinical depression. Our work deepens insights into social synchrony by simultaneous wireless sensing of peripheral biosignals. Concurrent monitoring of body temperature and brain activity while phenotyping ethologically relevant natural behavior offers a paradigm for monitoring the underlying mechanisms across the lifespan to reveal how early social interactions shape brain function (1-6).

Methods

All the methods are reported in accordance with ARRIVE guidelines.

Thermo-sensing devices

The thermo-sensor device was custom-designed and assembled (Fig. 1A & B), then double-coated with parylene and silicone impression material (EXACLEAR, G.C. Co., Ltd.) for waterproofing. The device was validated using a platinum resistance thermometer (MC-0403, Pt100 ClassA, Netsushin, Japan) and 4-wired RTD data acquisition module (NI-9217, National Instruments). Body temperature was measured every 30 s and the

data was saved on the device. As a battery lasts more than a few months, body temperature was recorded until the memory was full (~10 days). Data from the device were extracted and refreshed periodically via a wireless Bluetooth connection while the implant remained subcutaneous in the animal.

Experimental models and Experimental methods

Experiments were performed in accordance with experimental protocols approved by the Animal Experimentation Committee of the Medical School of The University of Tokyo.

Mice: Adult mice (C57Bl6/J) were purchased from a local provider (CLEA Japan, Inc.) and housed individually in a transparent plastic cage (320 × 210 × 130 mm (W × D × H); CLEA Japan, Inc.) until surgery. Three pairs of adult male mice (3–6 months old, 26.6−32.8 g, BW) were subcutaneously implanted with the thermo-sensor device on their back, thoracic region close to the mid-line under gas anesthesia (Isoflurane 2–3%). An incision was made in the skin, and the entire thermo-sensor device inserted subcutaneously, and then the incision stitched shut. After sensor implantation, mice were individually housed for two days. Immediately after recovering from anesthesia (~5 minutes), mice started to behave normally in the cage. On the third day, they were introduced into the same cage and housed together in a sound attenuation chamber (Muromachi) for the next 3–8 days. Room temperature and light cycle were set at 25°C and 12hL/12hD (light on at 8:00), respectively. Mouse behaviors were monitored by IR camera (FLIR

Grasshopper 3 Camera GS3-U3-41C6, Edmund Optics) from the cage top and data saved on the PC.

Zebra finches: Zebra finches were hatched and raised in our colony. They were raised by their parents with their siblings (if any) until ~ 60 days post hatch, when they were moved to a holding cage where only other zebra finches of the same sex were raised (5−15 birds/cage). A pair of sexually mature (> 6 month old) male and female adults unfamiliar to each other was randomly selected and housed in a cage equipped with a nest within a sound attenuation chamber (MODEL MC-050, Muromachi).

We used five pairs, with one female paired with two males sequentially (five pairs with four females and five males, 173–935 days post hatch, 13.5−15.5 g, BW). All birds, except one female, had no previous mating experience. One female had one mating experience with a male not used in this study. Cages with the same configuration (370 × 415 × 440 mm (W × D × H); HOEI, Japan) for breeding, holding, and pairing were used. Cages had two perches and a wired floor with water and food provided *ad libitum*. After 1 or 34 days pairing in the same cage, the birds of a pair were subcutaneously implanted with the wireless thermo-sensor device on their backs under local anesthesia (Xylocaine Jelly 2%, Sandoz Pharma K.K.).

Xylocaine jelly was spread on the back covering the area where the sensor device was to be implanted (~1.5 cm long). An incision was made in the skin, and the entire thermo-sensor device inserted subcutaneously while the bird was held by hand, then the incision was glued shut (Aron Alpha A,

Sankyo). Surgery was rapidly completed (within minutes), and birds behaved normally in the cage immediately after being released. The thermo-sensor devices recorded zebra finch body temperatures every 30 s, and the recorded data were extracted via Bluetooth signals every several days. Body temperature was recorded for 8−19 days with or without gaps (3−10 days continuously) (Supplemental Table 1). Their behavior was constantly monitored in a sound attenuation chamber using two video cameras (Webcam, Logicool) which sat beside and in front of each cage, respectively, and one IR camera focused inside the nest and recorded on a PC (Dell). Room temperature and light cycle were set at 25°C and 14hL:10hD (light on at 7:00), respectively to keep the birds in breeding condition.

Data Analysis

All analyses were performed using MATLAB (MathWorks), unless otherwise stated. Spearman correlations of body temperature fluctuations between a pair of mice/zebra finches over one day (24 hours) starting at lights-on were analyzed. To see the synchrony of body temperature between mouse pairs, the correlation coefficients before and after mouse pairs were co-housed (i.e., in separate cages vs in the same cage) were compared. For birds, the correlation coefficients of co-housed bird pairs were compared with those between birds that were recorded at the same time in different cages (e.g., a male bird in cage 1 and a female bird in cage 2). As each cage was isolated in a sound attenuation chamber, the birds in different cages could not see or hear each other.

To avoid the effect of circadian drift, correlation was measured between the delta body temperature: Time series data of body temperature for one day were averaged among all recording days for each animal (mice: 2–7 days, zebra finches: 8–19 days). Then the time series of body temperature for each day was subtracted by the average (delta body temperature). To avoid the effect of switching lights on and off, the data within one hour after light off/on were excluded. Then, Spearman correlations of delta body temperature between a pair were calculated for each day. To compare the correlation coefficient between light and dark periods for each day, Spearman correlations of delta body temperature from one hour after switching lights on to one hour before turning off and one hour after switching light off to one hour before turning on were calculated, respectively.

Video analysis for movement during sleep period

Video data for one light period for mice and dark period for birds were extracted and down-sampled to 15 frames per second with WonderShare (Filmora). One image per second was read as a greyscale frame in MATLAB. The difference between two adjacent frames as a summation of pixel differences was calculated to detect movement of a mouse or bird. As we found that the bird pairs spent almost all their dark time in the nest, we only used video frames from the IR camera focused inside the nest.

To match body temperature data, the frame differences were summed for 30 s. For a mouse pair, the period when frame differences were higher than threshold, decided by visual inspection, was defined as the time both

mice moved together (Fig 4A). We then calculated Pearson correlation coefficients only for the periods when mice did not move during sleep (light condition) to determine whether higher correlations in the light phase might be attributable to simultaneous short waking bouts (Fig 4C left). We examined the original video to see if mouse pairs slept by huddling together when the frame differences were lower than threshold for >30 min. For birds, original video was examined to see if bird pairs stayed together in the nest, and Pearson correlation coefficients were calculated only for the nights (dark phase) for which we could confirm the bird pair stayed together to check whether lower correlations might be attributable to isolation (Fig 4C, right).

Statistical analysis

All statistical analysis was done with computer software, OriginPro (OriginLab) or R, except for calculating Spearman correlation coefficients. The latter was calculated between the body temperature of two individuals measured at the same time in one day or light and dark time, respectively in one day with MATLAB code. To compare body temperature synchrony between pairs and unpaired individuals, we performed a linear mixed models (LMMs) analysis in which the correlation coefficients were response to a variable, and the pair condition (separate vs same cage for mice, pair vs shuffled for birds) was a fixed effect, and the individual pairs was a random effect. To compare body temp synchrony between light and dark condition, the LMMs were applied to mouse and bird pairs, respectively, in which the correlation coefficient was a response variable, the time (light vs dark) was a

fixed effect, and the individual pairs and the duration of pairing were a random effect. These LMMs were computed using R software v.4.5.2. (21) with packages lme4 (22) and lmerTest (23).

Funding statement declaration

This study was supported by a KICKS grant from OIST Graduate University to TKH and YY-S; JSPS KAKENHI (18H02531, 22H04767, 24H02316) to YY-S; and JSPS WPI-IRCN.

References

1. L. A. Eales The influences of visual and vocal interaction on song learning in zebra finches. *Animal Behaviour,* **37**, 507–508 (1989).
2. S. Derégnaucourt *et al.,* How sleep affects the developmental learning of bird song. *Nature* **433**, 710–716 (2005).
3. V. Leong *et al.,* Speaker gaze increases information coupling between infant and adult brains. *PNAS* **114,** 13290-13295 (2017).
4. M. Teicher *et al.*, The effects of childhood maltreatment on brain structure, function and connectivity. *Nat Rev Neurosci* **17**, 652–666 (2016).
5. M. Niwa *et al.,* Vulnerability in early life to changes in the rearing environment plays a crucial role in the aetiopathology of psychiatric disorders, *International Journal of Neuropsychopharmacology* **14**, 459–477 (2011)

6. Y. Makino *et al.,* Sleep-sensitive dopamine receptor expression in male mice underlies attention deficits after a critical period of early adversity. *Sci Transl Med*. **16**, eadh97632024 (2024).
7. S. Haniffa *et al.*, Chronic social stress blunts core body temperature and molecular rhythms of *Rbm3* and *Cirbp* in mouse lateral habenula. *Open Biol*. **13**, 220380 (2023).
8. A.E. Mason *et al.*, Elevated body temperature is associated with depressive symptoms: results from the TemPredict Study. *Sci. Rep.*, **14**, 1884 (2024).
9. K. Stern and M. McClintock, Regulation of ovulation by human pheromones. *Nature* **392**, 177–179 (1998). https://doi.org/10.1038/32408
10. S.R. Lone and V.K. Sharma, Social synchronization of circadian locomotor activity rhythm in the fruit fly Drosophila melanogaster. *J Exp Biol.* **214**, 3742-2750 (2011). doi: 10.1242/jeb.057554. PMID: 22031738.
11. O. Siehler *et al.*, Social synchronization of circadian rhythms with a focus on honeybees. *Philos Trans R Soc Lond B Biol Sci.* **376**, 20200342 (2021). doi: 10.1098/rstb.2020.0342.
12. M.J. Paul *et al.*, Social forces can impact the circadian clocks of cohabiting hamsters. *Proc Biol Sci*. **281**, 20132535 (2014). doi: 10.1098/rspb.2013.2535.
13. N. Mrosovsky, Phase response curves for social entrainment. *J. Comp. Physiol.* **162**, 35–46 (1988). https://doi.org/10.1007/BF01342701

14. J.D. Levine *et al.*, Resetting the Circadian Clock by Social Experience in Drosophila melanogaster. *Science* **298**, 2010-2012 (2002). DOI:10.1126/science.1076008

15. L. Kingsbury *et al.*, Correlated neural activity and encoding of behavior across brains of socially interacting animals. *Cell* **178**, 429-446.e16 (2019).

16. W. Zhang, M.M. Yartsev, Correlated neural activity across the brains of socially interacting bats. *Cell* **178**, 413-428.e22, (2019).

17. M.I. Sotelo *et al.*, Neurophysiological and behavioral synchronization in group-living and sleeping mice, *Curr. Biol*. **34**, 132-146.e5 (2024).

18. C. Gilbert *et al.*, One for all and all for one: the energetic benefits of huddling in endotherms. *Biological Reviews* **85,** 545-569 (2010). https://doi.org/10.1111/j.1469-185X.2009.00115.x

19. A.J. Davidson and M. Menaker, Birds of a feather clock together – sometimes: social synchronization of circadian rhythms, *Curr. Opin. Neurobio.* **13**, 765-769 (2003). https://doi.org/10.1016/j.conb.2003.10.011.

20. N.M. Rzechorzek *et al.*, A daily temperature rhythm in the human brain predicts survival after brain injury. *Brain* **145**, 2031-2048 (2022).

21. R Core Team, R: A language and environment for statistical computing. *R Foundation for Statistical Computing, Vienna, Austria* (2020). https://www.R-project.org/

22. D. Bates *et al.*, Fitting Linear Mixed-Effects Models Using lme4. *Journal of Statistical Software* **67** 1–48 (2015). doi:10.18637/jss.v067.i01

23. A. Kuznetsova *et al.*, lmerTest Package: Tests in Linear Mixed Effects Models. *Journal of Statistical Software* **82** 1–26 (2017). doi:10.18637/jss.v082.i13

Resource availability

Lead contact: Yoko Yazaki-Sugiyama (yazaki-sugiyama@oist.jp)

Data availability: Datasets generated and/or analyzed during the current study are not publicly available due to the requirement of detailed annotation but are available from the corresponding author on reasonable request.

Code availability: Computer code generated during the current study for analyzing the data (MatLab code) are available from the corresponding author on reasonable request.

Acknowledgments

We thank Dr. Izawa for helping with statistical analysis, Dr. Neal A. Hessler for setting up video systems, and Ms. Atsuko Oba for experimental animal maintenance.

Author Contributions: Y. Y.-S., and T.K.H. designed the experiments; Y.Y.-S. and Y.M. conducted the experiments; R.I., Y.Y., Y.I., and K.M. designed and established the sensor devices; M.N. and S.T modified the sensor devices for

animal experiments; Y.Y.-S. analyzed the data with help from M.K.; Y.Y.-S. and T.K.H. wrote the paper.

Declaration of interests: Authors declare no competing interests.

Figure legends

Figure 1. Experimental design

A: Images of the thermo-sensor device with the image of 1 yen coin (20 mm diameter) for scale comparison (top). **B:** Technical drawing and **C:** Specifications Table of the thermo-sensor device.

Figure 2. Synchronized body temperature fluctuations between male mouse pairs.

A: Schematic of experimental design for mouse pairs. Body temperatures were continuously measured after sensor device implantation. **B:** Body temperature fluctuations in a pair of male mice housed in separate cages (left) or in the same cage (right). Shaded areas indicate the dark phase (lights off). **C:** Spearman correlation coefficient between daily body temperatures of mouse peers (left) (n = 3). Each plot represents data for one full day (24 h) with symbols of the same color and shape denoting the same pairs. The correlation was significantly higher when mice were housed together rather than apart (3 pairs, p = 0.0063, df = 14.98, t-value = 4.30, Linear mixed model fit by maximum likelihood, t-tests use Satterthwaite's method [lmerModLmerTest]). **D:** Spearman correlation coefficient of daily body

temperatures showed no significant change over the days after pairing ($p > 0.05$, $r^2 = 0.014$)**.**

Figure 3. Synchronized body temperature fluctuations between zebra finch mating pairs.

A: Schematic of experimental design in zebra finches. Body temperatures were continuously measured after sensor device implantation. **B:** Body temperature fluctuations in a male–female zebra finch pair housed together (left) or in different cages (right). Shaded areas indicate the dark phase (lights off). **C:** Spearman correlation coefficient between daily body temperatures of zebra finch pairs in the same cage (n = 5) or shuffled combinations of a male and a female recorded simultaneously in different cages (n = 5). Each plot represents data for one full day (24 h) with symbols of the same color and type denoting the same pairs. The correlation was significantly higher for mating pairs housed in the same cage rather than for male and female combinations across different cages (5 pairs vs 5 combinations, $p = 0.044$, df = 10.96, t-value = 2.28, Linear mixed model fit by maximum likelihood. t-tests use Satterthwaite's method [lmerModLmerTest]). **D:** Spearman correlation coefficient between daily body temperatures of zebra finch pairs revealed a linear correlation along

days after pairing for the group ($p = 0.025$ $r^2 = 0.079$), and for one individual pair (plots with green triangle: $p = 0.0049$, $r^2 = 0.38$).

Figure 4. Species-specific synchronization of body temperature during sleep **A:** Video image of mouse (left) and zebra finch (right) pairs during the light and dark phase, respectively. Representative plots of body temperatures and movements determined as differences between sequential video frame pixel values for one sleep period (light phase for mice, dark phase for birds). **B: Left**, Spearman correlation coefficient between body temperatures of three mouse pairs in the light and dark period over one circadian (24hr) cycle was significantly higher in the light (sleep) than in the dark (awake) ($p = 0.015$, df = 19.10, t-value = 2.67, Linear mixed model fit by maximum likelihood, t-tests use Satterthwaite's method [lmerModLmerTest]). Symbols match those in Fig. 2C, D. **Right**, Spearman correlation coefficient between body temperatures of five zebra finch pairs over one circadian (24hr) cycle was significantly higher in the light (awake) than in the dark (sleep) ($p < 0.0001$, df = 82.10, t-value = 5.22, lmerModLmerTest). Symbols match those in Fig. 3C, D. **C:** Distributions of Spearman correlation coefficients for all light phases (top, mice: asleep, birds: awake), and all dark phases (bottom) were significantly different for both species (mouse: $p = 0.021$, zebra finch: 9.46×10^{-4}, Kolmogorov–Smirnov [K-S] test). Correlation coefficient distribution for mouse pairs asleep without movement (middle) did not differ from that of the entire light phase ($p = 0.58$, K-S test); likewise for zebra finches asleep in the

nest compared to the entire dark phase (p = 0.98, K-S test), which was in turn lower than that of all light phases (p = 0.027, K-S test).

Figure 5: Difference in sleep synchrony of body temperature across species **A: Left,** Schematic of mouse pair sharing body temperature during sleep by huddling. **Right,** Body temperature of a male mouse pair around circadian light on-/offset indicated by dotted lines (data from 10 days). **B: Left,** Schematic of a zebra finch mating pair sleeping together with independent body temperature regulation. **Right,** Body temperature of a zebra finch mating pair anticipates circadian light on-/offset indicated by dotted lines (data from 13 days). **C:** A table of major differences in body temperature synchrony across species.

A

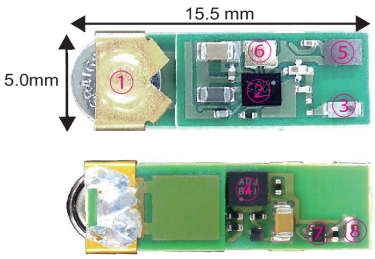

① Battery
② Microcomputer
③ BLE antenna
④ Thermo sensor
⑤ Non-volatile memory
⑥ Crystal oscillator
⑦ Optically triggered latch
⑧ LED

B

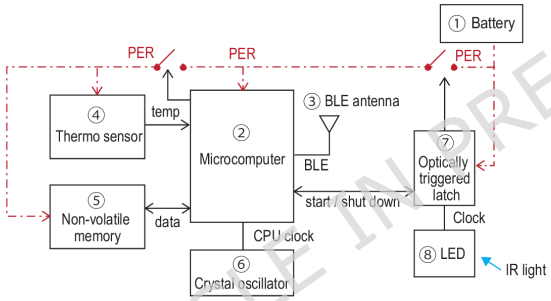

C

Temperature sensor	MAX30208 (Analog Devices)
Wireless communication	Bluetooth® 5.1, #DA14531 (Renesas)
Memory	64k byte
Battery	Silver Oxide (0.2g, OD:4mm) Battery life: > 6M

Size	15.5 × 5.0 × 2.70 mm
Weight	0.33 g (incl. battery)
Sensitivity	0.005 ± 0.1 deg

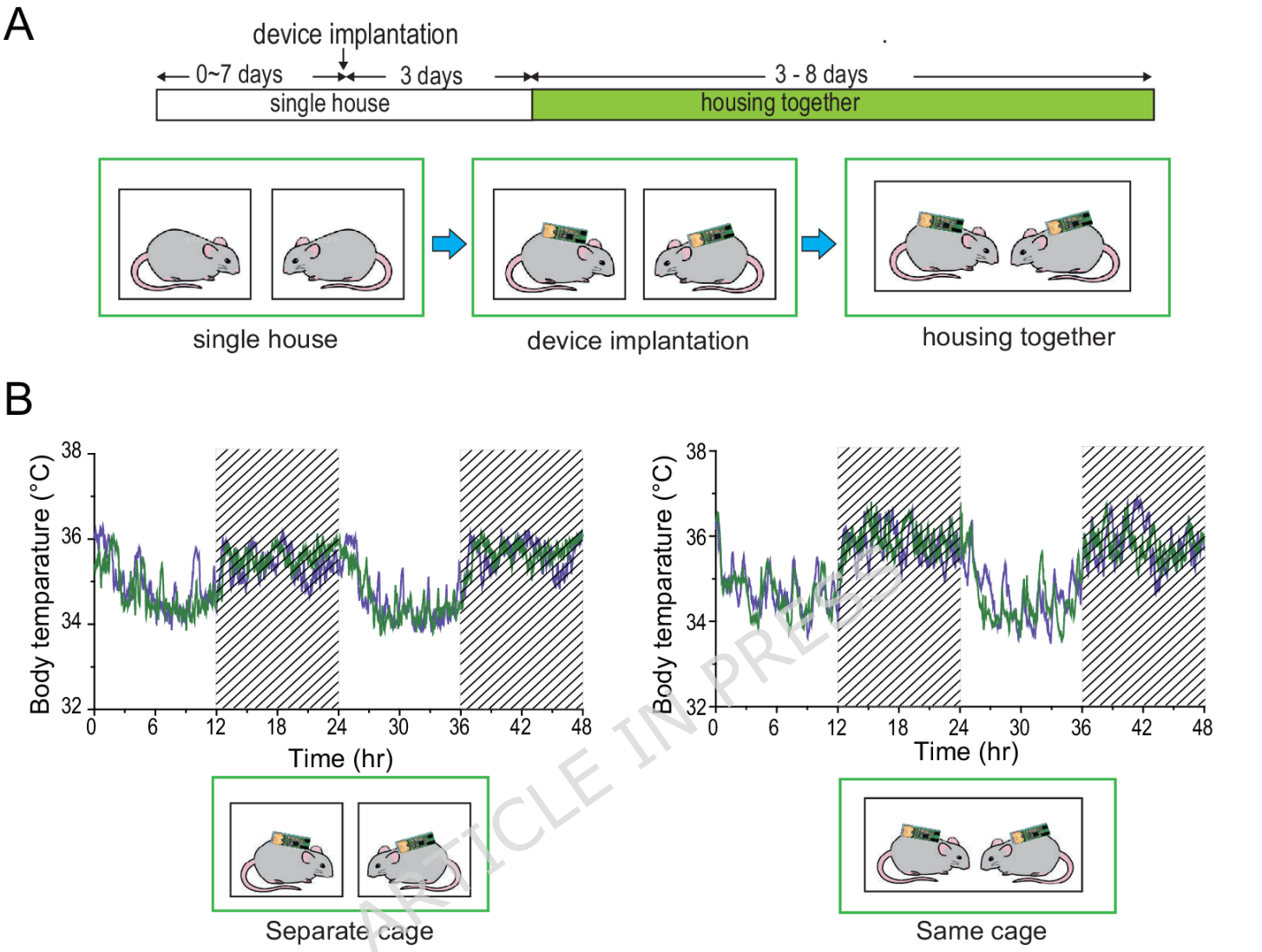

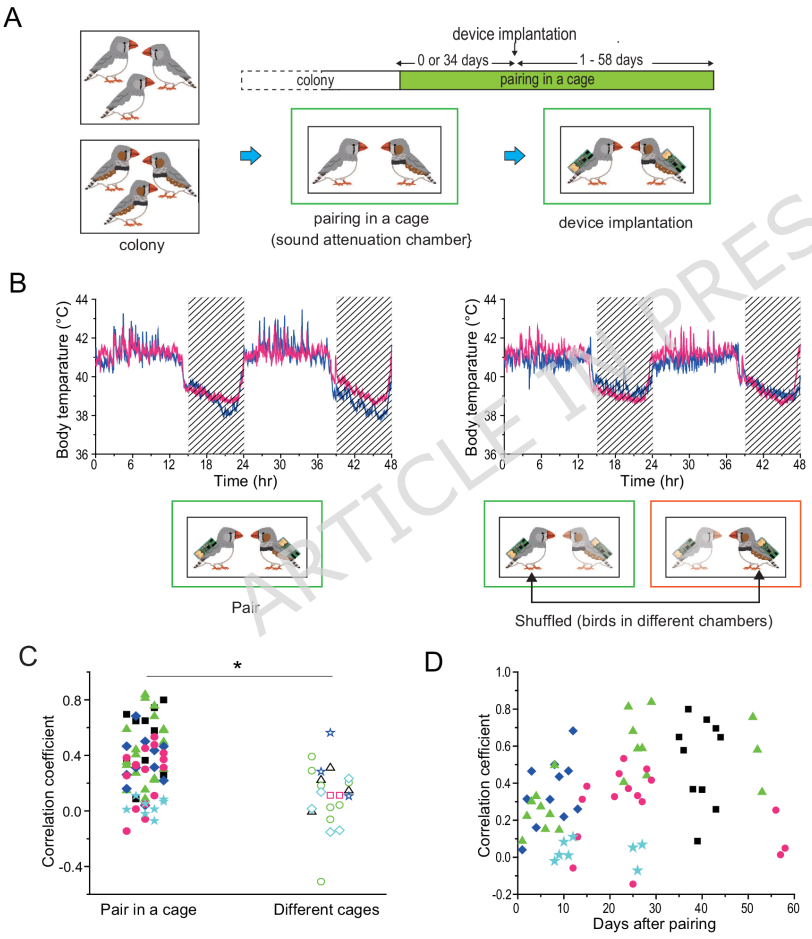

A

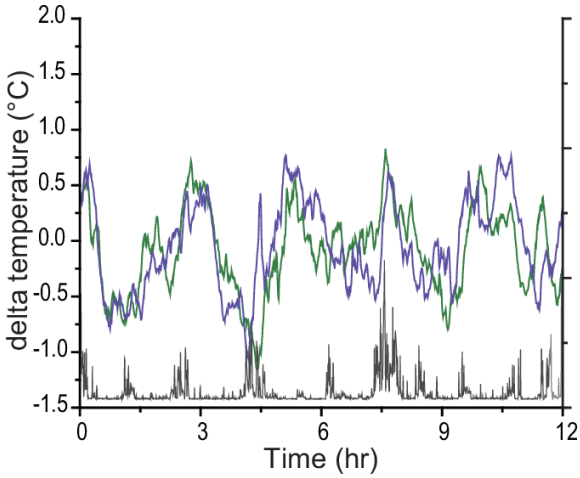

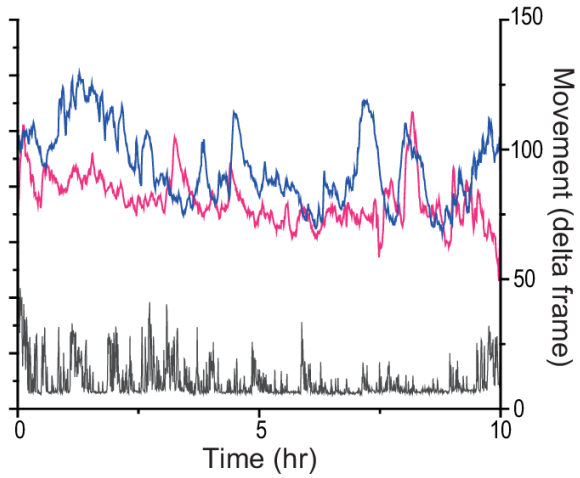

B

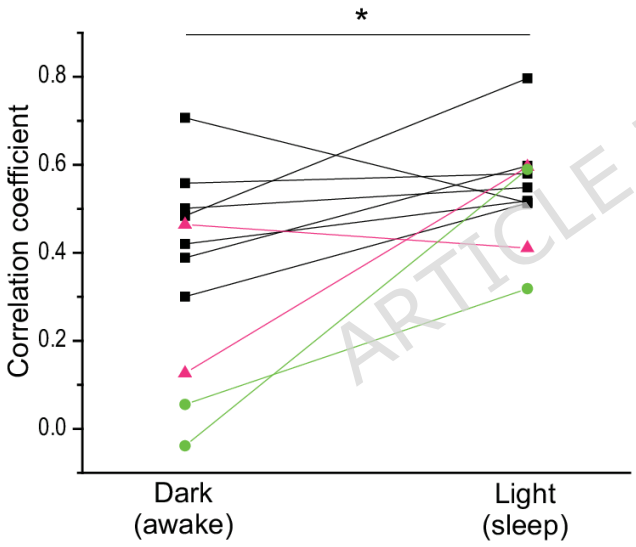

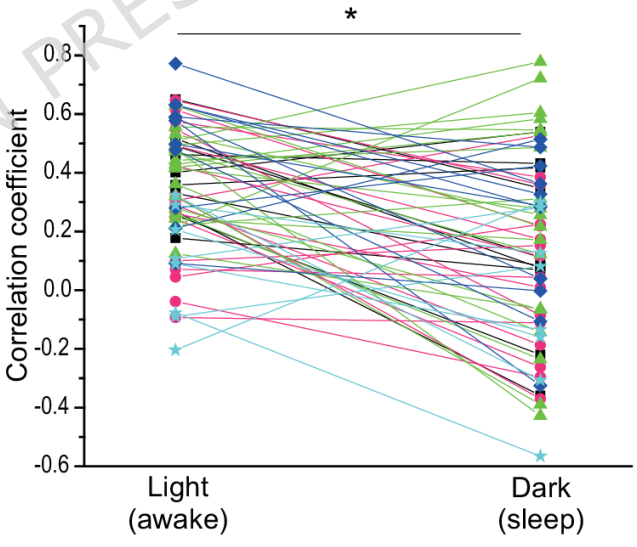

C

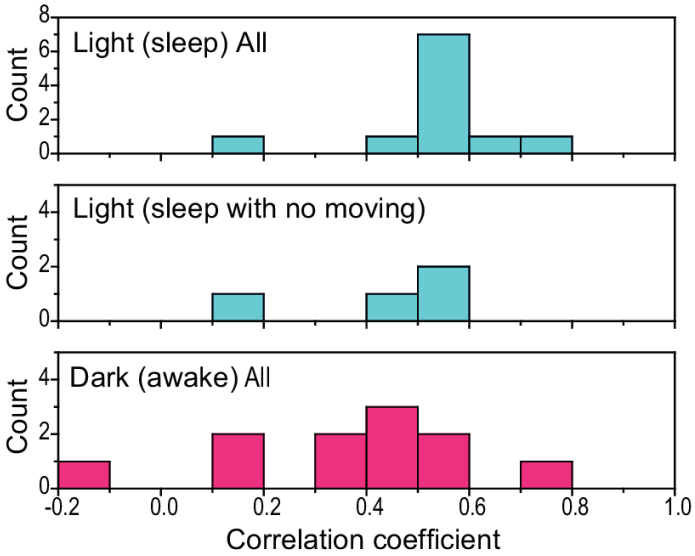

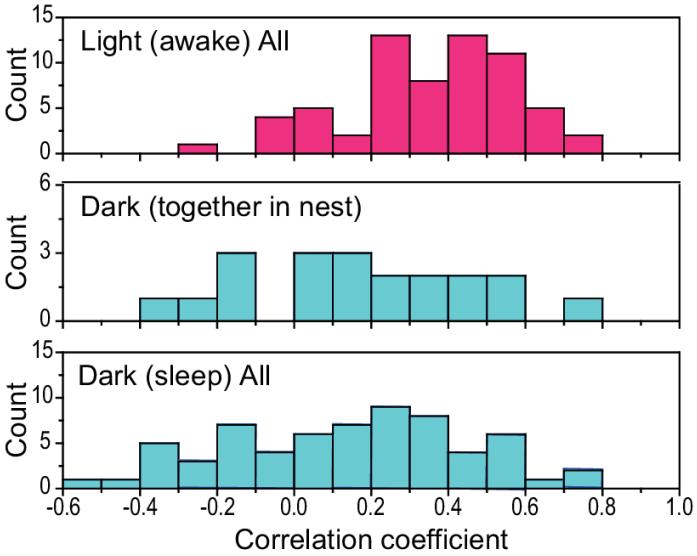

A

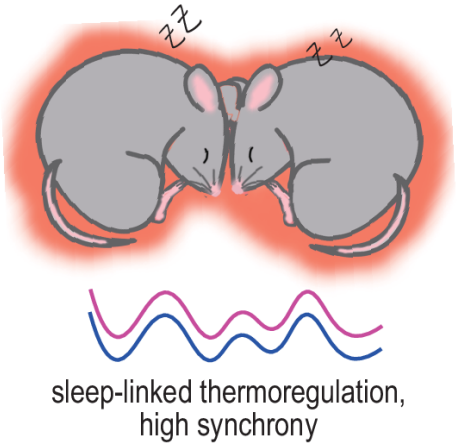

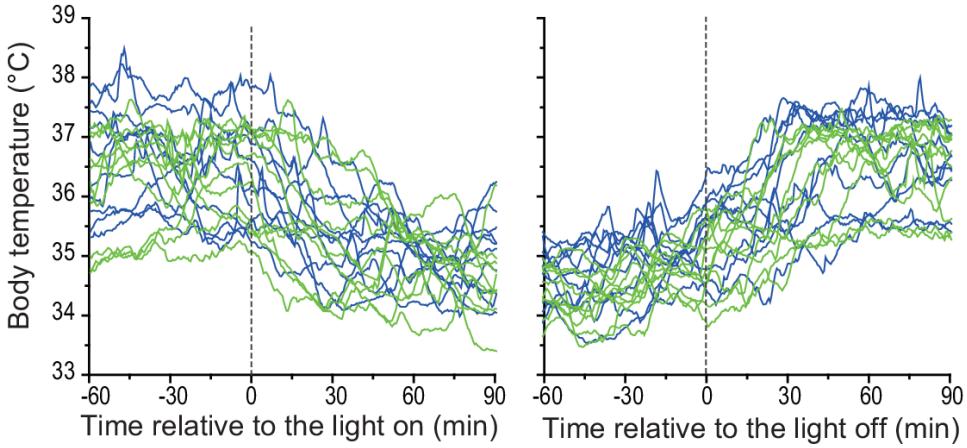

B

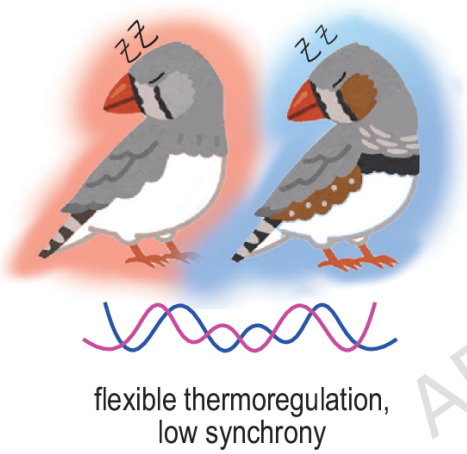

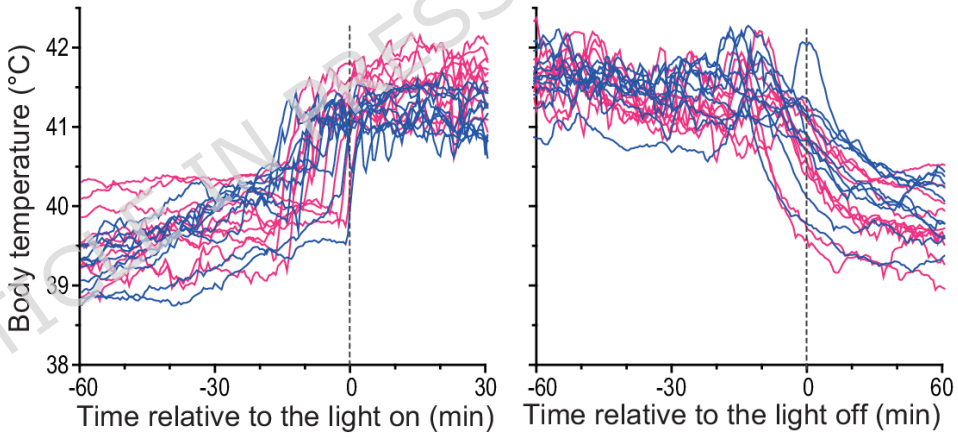

C

	Max synchrony	Anticipatory to light	Pairing duration for max synchrony
Mouse	Asleep	—	< 3 days
Bird	Awake	++	> 10 days